A New Optical Gain Model for Quantum Wells Based on Quantum Well Transmission Line Modelling Method

Xia, Mingjun; Ghafouri-Shiraz, Hooshang

DOI:
10.1109/JQE.2015.2396572

License:
Other (please specify with Rights Statement)

Document Version
Peer reviewed version

Citation for published version (Harvard):
Xia, M & Ghafouri-Shiraz, H 2015, 'A New Optical Gain Model for Quantum Wells Based on Quantum Well Transmission Line Modelling Method', *IEEE Journal of Quantum Electronics*, vol. 51, no. 3, 2500108. https://doi.org/10.1109/JQE.2015.2396572

A New Optical Gain Model for Quantum Wells Based on Quantum Well Transmission Line Modelling Method

Mingjun Xia and H. Ghafouri-Shiraz, *Senior Member, IEEE*

Abstract- This paper presents a new method for modelling the gain spectrum in quantum well structures based on the quantum well transmission line modelling (QW-TLM) method. In the QW-TLM method, three parallel RLC filters together with their associated weight coefficients constitute a QW-TLM unit, which represents the processes that electrons transit from the conduction band to the heavy hole band, the light hole band and the spin-orbit split-off band at a specific wave vector. Parallel QW-TLM units are adopted to describe the electron transitions in the wave vector space. Furthermore, the optical gain model of quantum wells based on the QW-TLM method is presented. The gain spectrum obtained through the QW-TLM method is agreeable with the gain spectrum calculated from the analytical expression in a large wavelength range from $1300nm$ to $1700nm$. In order to reduce the computation time, under sampling QW-TLM is proposed to model the gain curve of quantum wells. The simulation result shows that the gain curve obtained from under sampling QW-TLM is consistent with the gain curve obtained through the theoretical derivation from $1510nm$ to $1575nm$, which satisfies the requirement of studying the dynamic spectral characteristics of quantum well devices.

***Index items*-Quantum well, transmission line modelling, gain model, semiconductor optical devices, under sampling**

I. Introduction

Transmission line modelling (TLM) method was originally developed to solve field equations in microwave circuits [1]. In 1987, Lowery first presented the dynamic semiconductor laser model based on the TLM method [2] and since then this method was adopted to establish time domain models for Fabry Perot (FP) and distributed feedback (DFB) lasers as well as semiconductor optical amplifiers [2]-[5]. TLM has been found to be a useful method for modelling semiconductor optical devices particularly due to the ability of simulating the device spectra under modulation and providing a continuous spectral curve over a large bandwidth [6]. The wavelength dependent gain model based on the TLM method is an important tool for the analysis of spectral characteristics of both semiconductor lasers and amplifiers [6-7].

Manuscript received October 22nd, 2014. Revised Dec. 18th, 2014.This work was funded by both Dept. of EESE at the University of Birmingham and Chinese Scholarship council.

Mingjun Xia and Hooshang Ghafouri-Shiraz are with the Electronic, Electrical and System Engineering Department, University of Birmingham, Birmingham, B15 2TT, United Kingdom (e-mail: MXX322@bham.ac.uk; ghafourh@bham.ac.uk).

However, in quantum well structures, the gain spectrum curve is complex and asymmetric especially due to the hole's non-parabolic density of states and the coupling between the heavy hole bands, light hole bands and spin-orbit split-off bands in the presence of strain, which can't be modelled by a single filter [2], [5] or modified by adding another cascaded filter [8] as suggested for the bulk material semiconductor optical lasers and amplifiers. In Ref. [9], quantum well lasers including carrier transport effects were discussed using transmission line laser model, however, the author has assumed that the gain coefficient is wavelength independent. An accurate gain model for quantum well semiconductor optical devices using the TLM method enables us to analyse their spectral properties more accurately. In this paper, we have adopted the parallel QW-TLM units to model the electron transitions from the conduction band to the valence band in the wave vector space. Each QW-TLM unit consists of three RLC stub filters, which are used to describe the processes that electrons transit from the conduction band to the heavy hole band (HH), the light hole band (LH) and the spin-orbit split-off band (SO), respectively. The weight coefficient of each filter is determined by the values of the momentum matrix, the Fermi-Dirac distribution and the band energy in the corresponding wave vector.

We apply the QW-TLM method to analyse the optical gain model of quantum wells. Semiconductor optical devices are attractive in the high speed fiber communication systems and all-optical signal processing since they are energy efficient and easy to be integrated [10]-[16]. The evolution of the optical signal spectrum in the propagation is important to analyse the properties of quantum well devices. The common approach is to solve a set of rate equations for carrier and photon densities using one rate equation per longitudinal mode, but it needs a lot of computation time. Gain model of quantum wells based on QW-TLM provides an effective method to study the spectral characteristics in the process of optical signal propagation. Finally, under sampling QW-TLM method is proposed to further reduce the computation time.

This paper is organized as follows. The general theory of TLM is given in Section II. In section III, the QW-TLM method is introduced. Section IV presents the gain model for quantum wells based on the QW-TLM method; the gain spectrum obtained by the QW-TLM method is compared with the gain spectrum calculated through the analytical expression. Gain model of quantum wells using the under sampling QW-TLM

method is discussed in Section V. Finally, conclusions are given in section VI.

II. Transmission Line Modelling Theory

TLM is a time-discrete and space-discrete model of wave propagation [17], consisting of stub and link lines [18]. In the following first a brief review of the one-dimension TLM theory is presented. The input impedance, Z_{in} , of a lossless transmission line can be expressed as [19]:

$$Z_{in} = \frac{Z_0(Z_l + jZ_0 \tan(\beta l))}{Z_0 + jZ_l \tan(\beta l)} \quad (1)$$

where

$$\beta = \frac{2\pi f_0 n_g}{c_0} \quad (2)$$

In the above equations Z_0 is the characteristic impedance of the transmission line (TL), Z_l is the load impedance, l is the length of the TL, β is the propagation constant of the TL, n_g is the effective refractive index, c_0 is the light velocity in free-space and f_0 is the frequency of propagation wave. In order to make sure that all incident voltage pulses arrive at the scattering node at the same time, the length of the stub line should be such that the propagation time, ΔT , of the forward and backward pulses along the line satisfy the following expression [20]:

$$l = \frac{\Delta T c_0}{2n_g} \quad (3)$$

When a transmission line circuit is open- ($Z_l = \infty$) or short- ($Z_l = 0$) circuited their input impedances can be expressed as (see Eqs. (1) to (3)):

$$Z_{in-open} = Z_C / j \tan(\pi \Delta T f_0) \quad (4)$$

$$Z_{in-short} = jZ_L \tan(\pi \Delta T f_0) \quad (5)$$

where Z_0 in Eq.(1) is replaced by Z_C and Z_L which are the characteristic impedances of the open circuit and short circuit stubs, respectively. From the above equations we have:

$$\sqrt{Z_C / Z_L} = \tan(\pi \Delta T f_0) \quad (6)$$

In the TLM method (provided that $\Delta T < 1/2f_0$ or $f_{sam} > 2f_0$ where f_{sam} is the sampling frequency) a capacitor and an inductor can be represented by an open-circuit and a short-circuit stubs, respectively [20]. The Q-factor in a parallel RLC resonant circuit when the resistor is unity can be expressed as:

$$Q = \sqrt{C / L} \quad (7)$$

where the capacitor, C, and the inductor, L, can be obtained from Eqs.(4) and (5) as [20]:

$$C = \Delta T / 2Z_C \quad (8)$$

$$L = \Delta T Z_L / 2 \quad (9)$$

Substituting Eqs.(8) and (9) into Eq.(7) we have:

$$Q = 1/\sqrt{Z_C Z_L} \quad (10)$$

The characteristic admittance of the open and short circuit stubs can be obtained from Eqs. (4) to (10) as:

$$Y_C = Q / \tan(\pi \Delta T f_0) \quad (11)$$

$$Y_L = Q \tan(\pi \Delta T f_0) \quad (12)$$

III. TLM method for Quantum Wells

In quantum well semiconductor optical devices, the gain curve is dependent on the wavelength, carrier density and carrier temperature. The passive RLC filter shown in Fig.1(a) is commonly used to model the symmetric frequency-dependent gain curve [2]. The TLM model of this passive filter is shown in Fig.1(b) which consists of link and stub lines.

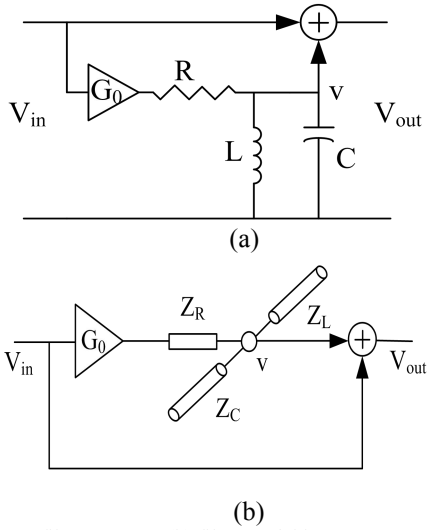

Fig. 1 (a) An RLC filter structure (b) filter model by TLM

In the TLM method the process of optical wave propagation is described through the connecting and scattering matrices [20]. However, as the gain spectrum of a quantum well structure is complex and asymmetric, we cannot use a single stub filter (see Fig.1(b)) to describe the complex processes in quantum well semiconductor optical devices. Therefore, we propose a new modelling method hereby referred to as the quantum well transmission line model (QW-TLM) to model the gain curve, which is dependent on the wavelength, carrier density and carrier temperature. The proposed model which represents the electron transitions in the wave vector space is referred to as the parallel QW-TLM units. Figure 2 shows one of the units which consists of three parallel stub filters and their corresponding weight coefficients A_1 , B_1 and C_1 .

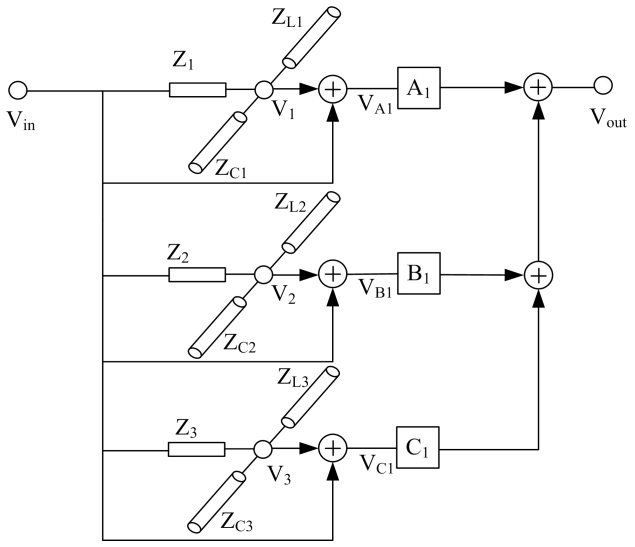

Fig. 2 A QW-TLM unit

In the above QW-TLM unit, stub filters shown in the 1st, 2nd and 3rd branches are used to describe the electron transition processes from the conduction band to the heavy hole, light hole and spin-orbit split-off bands at a specific wave vector, respectively. Axial approximation [21] is applied to simplify the electron transition process in the wave vector space. The resistor value in each branch of the unit is assumed to be unity (i.e. $Z_p = 1, p = 1,2,3$). Figure 3 describes the voltage propagation process in each stub filter. The input transmission line with the length Δl is used to represent the resistor while the open and short stub transmission lines each with length $\Delta l / 2$ are used to model the capacitor and inductor, respectively. In the time interval ΔT , the input voltage propagates along the input transmission line and arrives at the scattering node S and at the same period, the reflected voltages of the capacitor and inductor (V_C^r and V_L^r) propagate to the termination of the stub transmission lines and back again at the scattering node.

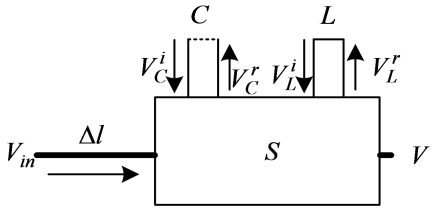

Fig. 3 Voltage propagation process in the stub filter

Based on the TLM theory, the Thevenin equivalent circuit of the stub filter is shown in Fig.4. The input currents of the node from the 1st 2nd and 3rd branches i_1 , i_2 and i_3 can be expressed as:

$$i_1 = V_{in} Y_R = V_{in} \tag{13}$$

$$i_2 = 2V_C^i Y_C \tag{14}$$

$$i_3 = 2V_L^i Y_L \tag{15}$$

The node voltage V can be expressed as

$$V = \frac{1}{Y}(i_1 + i_2 + i_3) = \frac{1}{Y}(V_{in} + 2V_C^i + 2V_L^i) \tag{16}$$

where,

$$Y = 1 + Y_C + Y_L \tag{17}$$

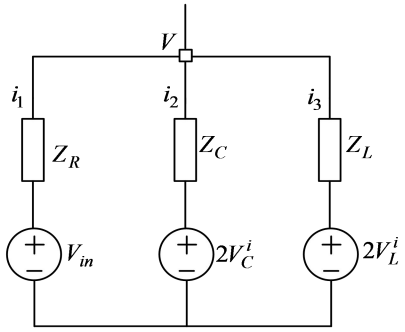

Fig. 4 Thevenin equivalent circuit of stub filter

Based on the above analysis, the node voltage of each stub filter (V_1 , V_2 and V_3) in the QW-TLM unit can be expressed as:

$$V_1 = \frac{1}{Y_1}(V_{in} + 2Y_{C1}V_{C1}^i + 2Y_{L1}V_{L1}^i) \tag{18}$$

$$V_2 = \frac{1}{Y_2}(V_{in} + 2Y_{C2}V_{C2}^i + 2Y_{L2}V_{L2}^i) \tag{19}$$

$$V_3 = \frac{1}{Y3}(V_{in} + 2Y_{C3}V_{C3}^i + 2Y_{L3}V_{L3}^i) \tag{20}$$

where,

$$Y_p = 1 + Y_{Cp} + Y_{Lp}, p = 1,2,3 \tag{21}$$

$$Y_{Cp} = \frac{1}{Z_{Cp}} = Q / \tan(\pi \Delta T f_p), p = 1,2,3 \tag{22}$$

$$Y_{Lp} = \frac{1}{Z_{Lp}} = Q \tan(\pi \Delta T f_p), p = 1,2,3 \tag{23}$$

In the above equations, V_{in} is the input voltage, (V_{C1}^i, V_{C2}^i , V_{C3}^i) and (V_{L1}^i , V_{L2}^i , V_{L3}^i) are the incident voltages of the capacitive and inductive stub lines, respectively, Y_{Cp} and Y_{Lp} are the characteristic admittances of the capacitive and inductive stub lines and f_p is the central frequency of the p[th] stub filter. The output voltage of each stub filter is:

$$V_{A1} = V_{in} + V_1 \tag{24}$$

$$V_{B1} = V_{in} + V_2 \tag{25}$$

$$V_{C1} = V_{in} + V_3 \tag{26}$$

and the output voltage of the whole QW-TLM unit is expressed as:

$$V_{out} = A_1 V_{A1} + B_1 V_{B1} + C_1 V_{C1} \tag{27}$$

The weight coefficients A_1 , B_1 and C_1 can be obtained from the QW momentum matrix, Fermi-Dirac distribution functions in the conduction and valence bands and the band structure. The voltages reflected into the capacitors, V_{Cp}^r , and inductors, V_{Lp}^r , of the QW-TLM unit can be expressed as:

$$V_{Cp}^r = V_p - V_{Cp}^i, p = 1,2,3 \tag{28}$$

$$V_{Lp}^r = V_p - V_{Lp}^i, p = 1,2,3 \tag{29}$$

These reflected voltages return and become new incident voltages after one iteration [7], that is:

$$ {}_{K+1}V^{i}_{Cp} = {}_{K}V^{r}_{Cp}, p = 1,2,3 \quad (30) $$

$$ {}_{K+1}V^{i}_{Lp} = -{}_{K}V^{r}_{Lp}, p = 1,2,3 \quad (31) $$

where, K is the iteration number.
In each stub filter, the capacitor and inductor frequency is a function of the wave vector k_t that can be expressed as:

$$ f_p(k_t) = (E^c_n(k_t) - E^{\upsilon}_{\sigma,m}(k_t))/h, \ \upsilon = HH, LH, SO \quad (32) $$

where, h is the Plank constant, $E^c_n(k_t)$ and $E^{\upsilon}_{\sigma,m}(k_t)$ are the energy band structure in the conduction and valence bands, respectively. When the heavy hole band energy ($E^{\upsilon}_{\sigma,m}(k_t)$, $\upsilon = HH$) is substituted into Eq. (32), we can obtain the central frequency of the first stub filter ($f_1(k_t), p = 1$). The band structures are obtained by solving the Schrodinger equations for the conduction and valence bands [21]-[23]:

$$ H^c \phi_n(z;k_t) = E^c_n(k_t)\phi_n(z;k_t) \quad (33) $$

$$ \sum_{\upsilon=HH,LH,SO} H^{\sigma}_{3\times3,i\upsilon} g^{\sigma}_{m,\upsilon}(z;k_t) = E^{\upsilon}_{\sigma,m}(k_t) g^{\sigma}_{m,i}(z;k_t) \quad (34) $$

where, H^c and $H^{\sigma}_{3\times3,i\upsilon}$ are the Hamiltonians for the conduction and valence bands, $\phi_n(z;k_t)$ is the envelope function of the *nth* conduction sub-band while $g^{\sigma}_{m,\upsilon}$ is the envelope function of the *mth* valence sub-band, σ denotes the upper and lower matrix signs in the block diagonal Hamiltonian for the valence band. In the Hamiltonians expression [21] we have considered the effects of both strain on the quantum well and the coupling between HH, LH and SO bands. The conduction band structure $E^c_n(k_t)$ is obtained by solving Eq. (33) at $k_t = 0$ and then using the following equation

$$ E^c_n(k_t) = E^c_n(k_t = 0) + \frac{\hbar^2 k_t^2}{2m_{e,t}} \quad (35) $$

where, $\hbar$ is the Plank constant divided by 2π , $m_{e,t}$ is the electron effective masses in the perpendicular to the growth direction. The valence band structure $E^{\upsilon}_{\sigma,m}$ is calculated by solving Eq. (34) using the finite difference method [22]. Due to spin orbit interaction, the valence band is spilt into the HH, LH and SO bands. Thus, in one QW-TLM unit, three stub filters are used to describe the processes electrons transit from the conduction band to heavy hole band, light hole band and spin-orbit split-off band at the same wave vector.

The Q-factor of each stub filter can be expressed as

$$ Q = 2\pi f_m / B \quad (36) $$

Where, f_m is the central frequency of the quantum well semiconductor optical device, B is the bandwidth of the stub filter, which is employed to describe the linewidth broadening caused by scattering.

IV. Gain Model of Quantum Wells

In the above analysis we introduced the quantum well transmission line modelling method, which can be applied to model different quantum well semiconductor optical devices. In the following, we analyse the gain model of quantum well and explain how to apply the QW-TLM method to model the gain function which is dependent on the wavelength, carrier density and temperature. In order to verify the validity of the QW-TLM method we first analyse the material gain of quantum wells and then compare the results with those obtained from the proposed QW-TLM method.

A. Band structure

At first, the conduction and valence bands of a strained $In_{0.64}Ga_{0.36}As$ - $InGaAsP$ quantum well are calculated by solving the Schrodinger equations (i.e. Eqs. (33) and (34)). The well and barrier widths are $4.5nm$ and $10nm$, respectively. The barrier with a band-gap wavelength $\lambda_g = 1.15\mu m$ is lattice-matched to the InP substrate. The parameters used in our model are given in Table 1-2 and some are taken from Ref. [24]. Figures 5(a) and (b) show the simulation results of the conduction and valence energy bands which are used to calculate the optical gain spectra. Curves labeled C1 and C2 in Fig. 5a represent the 1st and 2nd sub-bands in the conduction band and those in Fig.5b which are labelled HH1, HH2, LH1 and LH2 represent the first two sub-bands in the heavy hole and light hole bands. The strain effects and the coupling between the heavy hole, the light hole and the spin-orbit split-off bands have also been considered in the calculations.

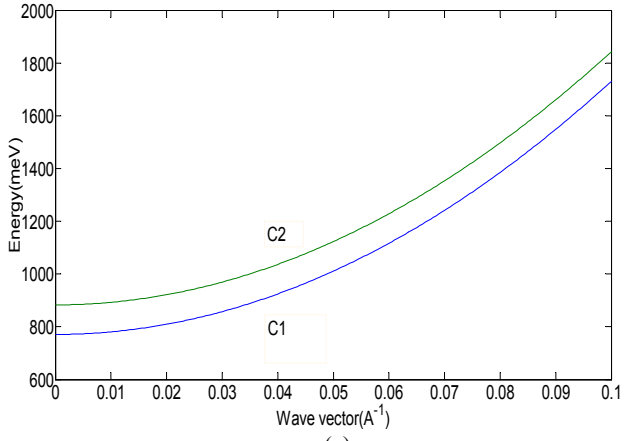

(a)

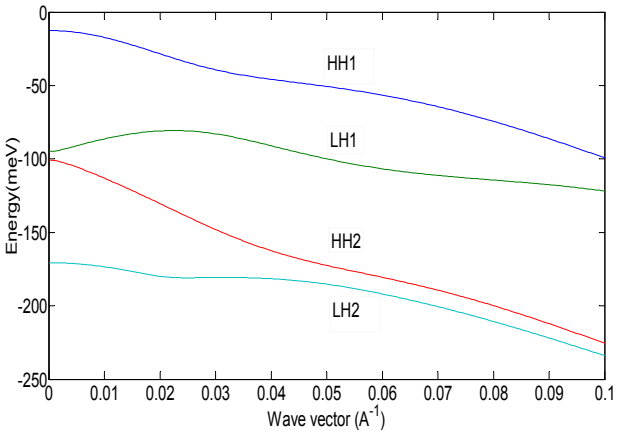

(b)

Fig. 5 (a) Conduction band structure (b) valence band structure of a compressively strained quantum well

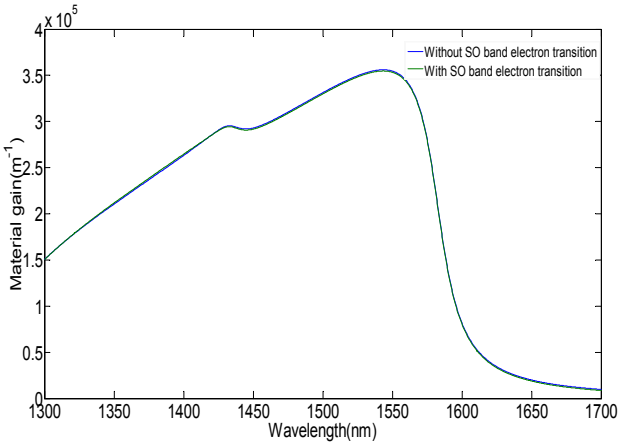

Fig. 6 Gain spectra of a strained quantum well in the presence and absence of spin-orbit split-off bands electron transition

B. Gain function of QWs based on Fermi's Golden Rule

The material gain $g(\omega)$ of quantum wells derived from the Fermi's golden rule can be expressed as [24]:

$$g(\omega)=\frac{q^2\pi}{n_r c_0 \varepsilon_0 m_0^2 \omega L_z}\sum_{\eta=\uparrow,\downarrow}\sum_{\sigma=U,L}\sum_{n,m}\int\left|\hat{e}\cdot M_{nm}^{\sigma\eta}\right|^2 \times\frac{(f_n^c(k_t)-f_{\sigma m}^{v}(k_t))(\hbar\gamma)}{4(E_{\sigma,nm}^{cv}(k_t)-\hbar\omega)^2+(\hbar\gamma)^2}\frac{k_t dk_t}{\pi^2} \quad (37)$$

where,

$$F_n^c(k_t)=1/[1+\exp(\frac{E_n^c(k_t)-E_{fc}}{K_B T})] \quad (38)$$

$$F_{\sigma m}^{\upsilon}(k_t)=1/[1+\exp(\frac{E_{\sigma,m}^{\upsilon}(k_t)-E_{f\upsilon}}{K_B T})] \quad (39)$$

$$E_{\sigma,nm}^{c\upsilon}(k_t)=E_n^c(k_t)-E_{\sigma,m}^{\upsilon}(k_t) \quad (40)$$

In the above equations, q is the magnitude of the electron charge, n_r is the ground refractive index, m_0 is the electron rest mass in free space, L_z is the quantum well width, ε_0 is the permittivity in free space and γ is line-width at half maximum of the Lorentzian function, $\hat{e}$ is the polarization vector of the optical electric field, $M_{nm}^{\eta\sigma}$ is the momentum matrix element, E_{fc} and $E_{f\upsilon}$ are the quasi-Fermi levels in the conduction and valence bands, respectively, K_B is the Boltzmann constant and T is the carrier temperature. Equation (37) is used to calculate the gain spectra of $In_{0.64}Ga_{0.36}As$ - $InGaAsP$ quantum well. The parameters used in the analysis are given in Table 1-2 and Ref. [24]. The simulation results both in the presence and absence of spin-orbit split-off bands electron transition are shown in Fig.6 which are in good agreement with those reported in Ref. [22]. As Fig.6 clearly indicates the electron transition from the conduction band to the spin-orbit split-off band has negligibly small effect on the material gain spectra of the quantum well due to its low energy level. Hence, its effect can be ignored.

Table 1
Parameters for the gain model

Symbol	Parameter	Value
Q	Stub filter Q-factor	60.8
Q_s	Compensation stub filter Q-factor	5
N	Carrier density	$8.0\times10^{24}\,m^{-3}$
f_{sam}	Sampling frequency	$1.0\times10^{15}\,Hz$
f_{usam}	Under sampling frequency	$6.2893\times10^{13}\,Hz$
b	Band number	3
r	Number of transform points	2048
γ	Linewidth of the Lorentzian function	$2\times10^{13}\,rad/s$
W_w	Well width	$4.5nm$
W_b	Barrier width	$10nm$
n_r	Background refractive index	3.67

Table 2
Quantum well material Parameters [24]

Parameters	Symbol	*InP*	*InAs*	*GaP*	*GaAs*
Lattice constant (A)	d	5.8688	6.0684	5.4512	5.6533
Band gap energy (eV)	E_g	1.344	0.354	2.78	1.424
Stiffness constants	C_{11}	10.220	8.329	14.120	11.880
($10^{11}\,dyn/cm^2$)	C_{12}	5.760	4.526	6.253	5.380
	γ_1	4.95	20.4	4.05	6.85
Luttinger Parameters	γ_2	1.65	8.3	0.49	2.1
	γ_3	2.35	9.1	1.25	2.9
Bir-Pikus deformation potentials (eV)	a_c	-5.04	-5.08	-7.41	-7.17
	a_v	-1.27	-1.00	-1.70	-1.16
Shear deformation potential (eV)	b	-1.7	-1.8	-1.7	-1.8
Spin-orbit splitting energy (eV)	Δ	0.11	0.38	0.08	0.34

C. Gain model of quantum wells based on QW-TLM

Figure 7 shows the material gain model for quantum wells which is based on the proposed QW-TLM method. The model consists of the gain coefficient G_0 and a number of parallel QW-TLM units. Each unit has two weight coefficients A_i and B_i, where, i denotes the branch number. Because the effect of the electron transition from the conduction band to the spin-orbit split-off band is negligible we have not included the 3rd branch of the QW-TLM unit (see Fig.2) in the proposed gain model shown in Fig.7.

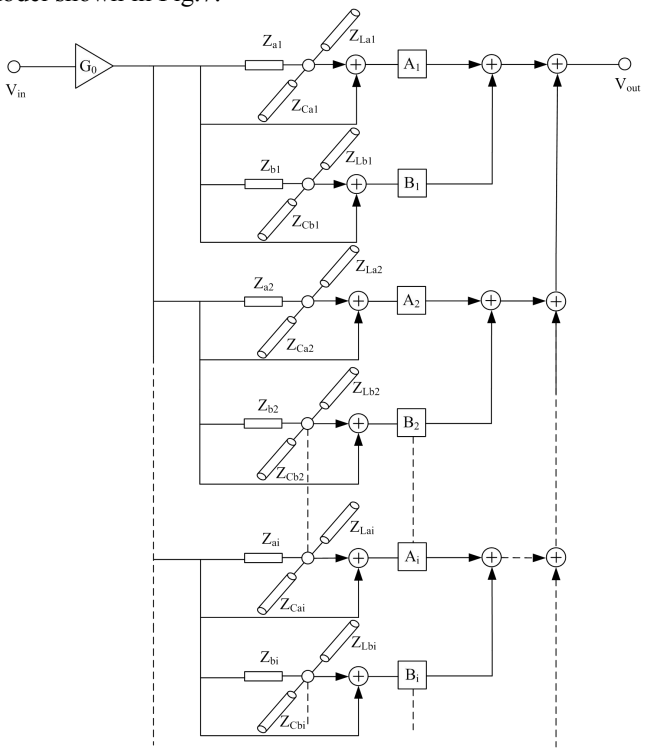

Fig. 7 Gain model of quantum wells based on QW-TLM

Referring to the *ith* QW-TLM unit in Fig.7, the 1st branch impedances Z_{ai}, Z_{Lai} and Z_{Cai} are resistors, inductors and capacitors, respectively, which are used to model the process that electrons in the conduction band transfer to the heavy hole band while the impedances in the 2nd branch Z_{bi}, Z_{Lbi} and Z_{Cbi} represents the process that electrons transfer from the conduction band to the light hole band. The frequencies for the 1st branch and the 2nd branch capacitors and inductors in the *ith* QW-TLM unit can be expressed as:

$$f_1(k_t(i)) = [E_n^c(k_t(i)) - E_{\sigma,m}^h(k_t(i))]/h \tag{41}$$

$$f_2(k_t(i)) = [E_n^c(k_t(i)) - E_{\sigma,m}^l(k_t(i))]/h \tag{42}$$

In the above equations $E_n^c(k_t(i))$ is the *nth* conduction band energy at the wave vector $k_t(i)$, $E_{\sigma,m}^h(k_t(i))$ and $E_{\sigma,m}^l(k_t(i))$ are the *mth* heavy-hole and light-hole band energies at the wave vector $k_t(i)$, respectively. The characteristic admittance values in *ith* QW-TLM unit can be obtained by substituting $f_1(k_t(i))$ and $f_2(k_t(i))$ into Eq. (22) to (23).The time interval ΔT in Eq. (22) and Eq. (23) can be expressed as:

$$\Delta T = 1/f_{sam} \tag{43}$$

where, f_{sam} is the sampling frequency which can be determined by the following expression:

$$f_{sam} \geq 2\max[f_1(k_t(i)), f_2(k_t(i))] \tag{44}$$

The weight coefficients A_i and B_i are given as

$$A_i = \frac{1}{f_1(k_t(i))}\left|\hat{e}M_{nm}^{\sigma\eta}(k_t(i))\right|^2 \times [F_n^c(k_t(i)) - F_{\sigma m}^h(k_t(i))]k_t(i)dk_t \tag{45}$$

$$B_i = \frac{1}{f_2(k_t(i))}\left|\hat{e}M_{nm}^{\sigma\eta}(k_t(i))\right|^2 \times [F_n^c(k_t(i)) - F_{\sigma m}^l(k_t(i))]k_t(i)dk_t \tag{46}$$

Where, $M_{nm}^{\eta\sigma}(k_t(i))$ is the momentum matrix element in the wave vector $k_t(i)$, dk_t is the wave vector interval in the numerical calculation, $F_n^c(k_t(i))$ is the value of the Fermi-Dirac distribution function for the conduction band in the wave vector $k_t(i)$, the values of the Fermi-Dirac distribution functions for the heavy hole, $F_{\sigma m}^h(k_t(i))$, and the light hole, $F_{\sigma m}^l(k_t(i))$, bands can be calculated from Eq. (39).

In order to calculate the Q-factor given in Eqs.(22) to (23) we equate the parameter γ which represents the full width at half maximum of the Lorentzian function given in Eq.(37) to the stub filter bandwidth B given in Eq.(36) which results in:

$$Q = 2\pi f_m / \gamma \tag{47}$$

D. Simulation Results

In the following section, we simulate the gain spectra of a compressively strained quantum well using the above two methods, the analytical expression derived from Fermi's golden rule (i.e. Eq.(37)) and the QW-TLM method. The two gain spectra are compared to verify the validity of the proposed QW-TLM method. The gain spectra of the proposed model can be obtained by applying FFT to the pulse sequence of the output node when a unit impulse is applied to the input node of the gain model (see Fig.7).

Figure 8 shows the normalized gain spectra obtained using both the analytical expression and the proposed QW-TLM method. As the results clearly indicate, the gain spectra obtained by the proposed model is in a very good agreement with that obtained by the analytical expression given in Eq. (37) within *1300nm* and *1700nm* wavelength band. In order to reduce the computation time we have assumed that the Q-factor in the proposed model is the same for all units and this has caused a negligibly small difference between the two methods within 1585 *nm* and 1670 *nm* wavelength band.

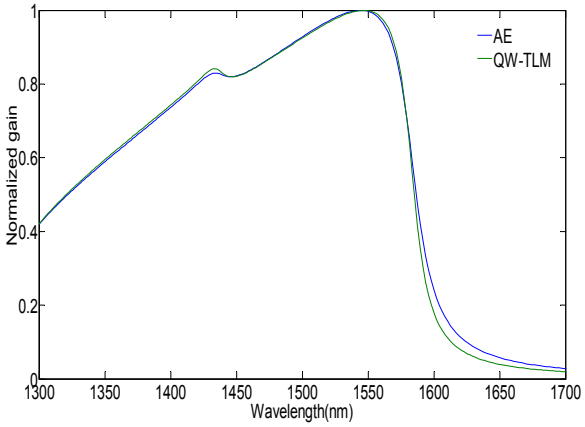

Fig. 8 Normalized gain spectra of a compressively strained quantum well based on the analytical expression (AE) and QW-TLM method

It should be noted that the sampling frequency f_{sam} used in the above analysis is in order of $10^{15} Hz$ which means the time step $\Delta T = 1/f_{sam}$ is very small and consequently the computation time is high in particular when the proposed QW-TLM method is used to analyse the dynamic behaviour of quantum well devices (about a few hours depending on the QW device parameters). However, in this work it took about 1min to obtain the gain spectra of the QW device. In order to minimise the computation time, a technique of sampling below the optical frequency (i.e. under sampling) is proposed in the following section. It worth's to note that the under sampling method has very little effect on the computation time when calculating gain spectrum of quantum wells, However, it reduces the computation time significantly when analyzing other characteristics of quantum well devices such as amplification of ultra-short pulses, dynamic spectral effects and so on.

V. Under Sampling QW-TLM

According to Ref [2] since the laser beam spectral linewidth Δf_m is very narrow as compared with its operating frequency f_m (typically 1%) the sampling frequency f_{sam} may be lowered without loss of information. To reduce modelling time f_{sam} should be minimised without any information loss within Δf_m. Let us denote f_{u-sam} and Q_u as the under sampling frequency and Q-factor. We have:

$$Q_u = Q(1 - b f_{u-sam} / f_m) \tag{48}$$

where f_m is the central frequency of the quantum well gain spectra, which can be obtained from Eq. (37) and b is an integer representing the band number and can be obtained from the following expression [2]:

$$b \le \frac{\min[f_1(k_t(i)), f_2(k_t(i))]}{2\{\max[f_2(k_t(i))] - \min[f_1(k_t(i))]\}} \tag{49}$$

In the under sampling method, the central frequencies of the parallel stub filters will decrease by subtracting $b f_{u-sam}$. Thus to minimise the error we have modified the gain model shown in Fig.7 by cascading it with a compensation stub filter as shown in Fig.9.

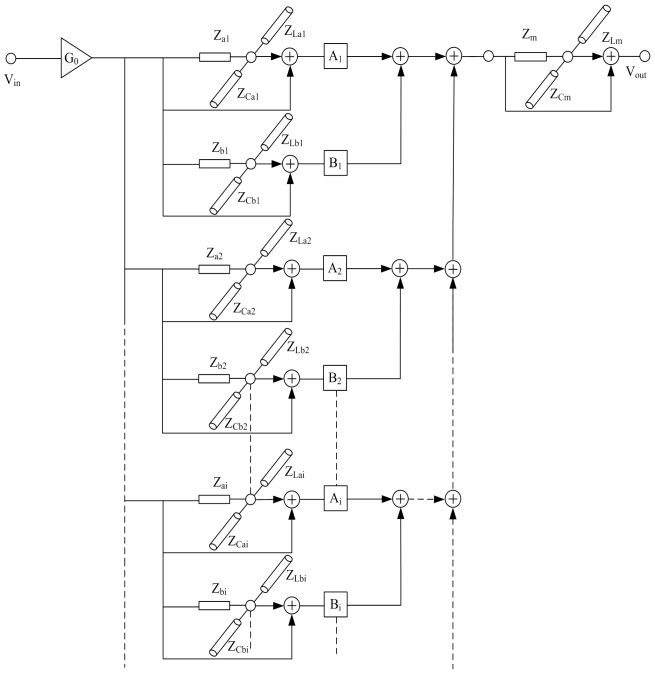

Fig. 9 Gain model of quantum wells using under sampling QW-TLM

This compensation stub filter has the following impedances (admittances):

$$Z_s = 1 \tag{50}$$

$$Y_{Cs} = \frac{1}{Z_{Cs}} = \frac{Q_{us}}{\tan(\pi f_{us} \Delta T)} \tag{51}$$

$$Y_{Ls} = \frac{1}{Z_{Ls}} = Q_{us} \tan(\pi f_{us} \Delta T) \tag{52}$$

Where

$$Q_{us} = Q_s(1 - b f_{u-sam} / f_m) \tag{53}$$

$$f_{us} = f_m - b f_{u-sam} \tag{54}$$

where, Q_s is the Q-factor in the compensation filter. Fig. 10 shows the normalized gain spectra of the strained quantum well obtained by both the under sampling QW-TLM method (i.e. Fig.9) and the analytical method given in Eq. (37) from $1510nm$ to $1575nm$. The results confirm that the gain spectra obtained by the proposed model is in a very good agreement with that obtained using the analytical expression. Hence, the under sampling QW-TLM method can be applied to analyse the dynamic spectral characteristics of quantum well optical semiconductor devices.

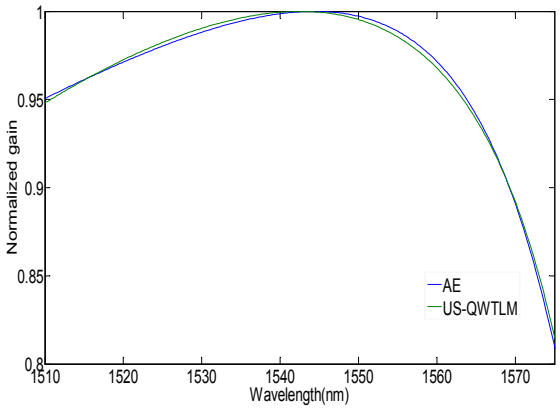

Fig.10 Normalized gain spectra of a compressively strained quantum well based on analytical expression (AE) and under sampling QW-TLM (US-QWTLM)

VI. CONCLUSION

In this paper, we have introduced a new method hereby referred to as the quantum well transmission line modelling method (QW-TLM) which is used to model the gain spectra of the quantum well semiconductor optical devices. The method consists of a number of QW-TLM units which are connected in parallel to model the electron transitions in the wave vector space. Each QW-TLM unit consists of three RLC stub filters and their corresponding weight coefficients, which represent the processes that electrons transit from the conduction band to the heavy hole band, the light hole band and the spin-orbit split-off band at a given wave vector. Explicit expressions for the admittances of the stub filters and the weight coefficients of each unit are provided. The simulation results indicate a very good agreement between the gain spectra obtained by the QW-TLM method and that obtained by the analytical expression within the wavelength band of $1300nm$ to $1700nm$.

Also, in order to reduce the computation time the under sampling QW-TLM method has been introduced where a cascaded RLC stub filter is added to the output of the gain model based on QW-TLM. The simulation results of the gain spectra of a stained quantum well using this model and the analytical expression are in a very good agreement within the wavelength band of $1510\,nm$ to $1575nm$.

The QW-TLM method is an effective approach that enables us to analyse the dynamic spectral characteristics of quantum well semiconductor optical devices.

REFERENCES

[1] P.B. Johns and R.L. Beurle, "Numerical solution of 2-dimensional scattering problems using a transmission-line matrix," IEE Proc. J., vol.188, no. 9, pp. 1203-1208, 1971.

[2] A.J. Lowery, "New dynamic semiconductor laser model based on the transmission line modelling method," IEE Proc. J., vol. 134, pp.281-290, 1987.

[3] W. M. Wong and H. Ghafouri-Shiraz, "Integrated semiconductor laser-transmitter model for microwave-optoelectronic simulation based on transmission-line modelling," IEE Proc. J.,, vol. 146, no. 4, pp. 181-188, 1999.

[4] W. M. Wong and H. Ghafouri-Shiraz, "Dynamic model of tapered semiconductor lasers and amplifiers based on transmission line laser modeling," IEEE Jour. Select. Top. Quant. Elec., vol. 6, no. 4, pp. 585-593, 2000.

[5] A.J. Lowery, "New inline wideband dynamic semiconductor laser amplifier model," IEE Proc. J., vol. 135, no. 3, pp. 242-250, 1988.

[6] A.J. Lowery, "Transmission-line modelling of semiconductor lasers: the transmission-line laser model," International Journal of Numerical Modelling, vol. 2, pp. 249-265, 1989.

[7] A.J. Lowery, "Modelling spectral effects of dynamic saturation in semiconductor laser amplifiers using the transmission-line laser model," IEE Proc. J., vol. 136, no. 6, pp. 320-324, 1989.

[8] A.J. Lowery, "Efficient material-gain models for the transmission-line laser model," International Journal of Numerical Modelling., vol. 2, pp. 249-265, 1989.

[9] L. V. T. Nguyen, A. J. Lowery, P. C. R. Gurney and D. Novak, "A time-domain model for high-speed quantum-well lasers including carrier transport effects," IEEE J. Select. Topics Quantum Electron., vol. 1, pp.494–504, 1995.

[10] P.W. Juodawlkis, J. J. Plant, W. Loh, L. J. Missaggia, K. E. Jensen and F. J. O'Donnell, "Packaged $1.5\mu m$ Quantum-Well SOA with 0.8-w output power and 5.5-dB noise figure," IEEE Photon. Technol. Lett., vol. 21, no. 17, pp. 1208–1210, Sep. 2009.

[11] X. Huang, Z. Zhang, C. Qin, Y. Yu, and X. Zhang, "Optimized quantum–well semiconductor optical amplifier for RZ-DPSK signal regeneration," IEEE J. Quantum Electron., vol. 47, no. 6, pp. 819–826, Jun. 2011.

[12] Amir Capua, Ouri Karni, Gadi Eisenstein and Johann Peter Reithmaier, "Rabi oscillations in a room-temperature quantum dash semiconductor optical amplifier," Phys Rev B, vol. 90, pp. 045305, 2014

[13] Hiroki Ikehara, Tsuyoshi Goto, Hiroshi Kamiya, Taro Arakawa and Yasuo Kokubun, "Hitless wavelength-selective switch based on quantum well second-order series-coupled microring resonators," Opt. Express, vol. 21, no. 5, pp.6377-6390, Mar. 2013.

[14] O. Qasaimeh,"Analytical model for cross-gain modulation and crosstalk in quantum-well semiconductor optical amplifiers,"Lightw. Technol., vol. 26, no. 4, pp. 449–456, Feb. 2008.

[15] Jijun Feng, Ryoichi Akimoto, Shin-ichiro Gozu, and Teruo Mozume, "All-optical XOR logic gate using intersubband transition in III-V quantum well materials," Opt. Express, vol. 22, no. 11, pp.12861-12868, May, 2014.

[16] Capua, A. et al. Coherent control in a semiconductor optical amplifier operating at room temperature. Nat. Commun. 5:5025 doi: 10.1038/ncomms6025 (2014).

[17] P. B. Johns, "A new mathematical model to describe the physics of propagation," Radio Electron. Eng., vol. 44, pp. 657-666, 1974.

[18] J. W. Bandler, P. B. Johns, and M. R. M. Rizk, "Transmission-Line Modeling and Sensitivity Evaluation for Lumped Network Simulation and Design in the Time Domain," Jour. Frank. Inst., vol. 304, pp. 15-32, 1977.

[19] R. E. Collins, Foundations of Microwave Engineering. New York: McGraw-Hill, 1966.

[20] P.B. Johns and M. O'Brien, "Use of the transmission-line modelling (TLM) method to solve non-linear lumped networks," Radio & Electron. Eng., vol. 50, pp. 59-70, 1980.

[21] C. Y -P. Chao and S. L. Chuang, "Spin-orbit-coupling effects on the valence-hand structure of strained semiconductor quantum wells," Phys Rev E, vol. 46, pp. 411M122, 1992

[22] C. Chang and S. Chuang, "Modeling of strained quantum-well lasers with spin-orbit coupling," IEEE J. Sel. Topics Quantum Electron., vol. 1, no. 2, pp. 218–229, Jun. 1995.

[23] M. Sugawara, N. Okazalu, T. Fujii, and S. Yamazalu, "Conduction-band and valence-band structures in strained InGaAs/InP quantum wells on (001) InP substrates,'' Phys. Rev E, vol. 48, pp. 8102-8118, Sep. 1993.

[24] S. L. Chuang, Physics of Optoelectronic Devices. New York: Wiley, 1995.

Author introduction

Mingjun Xia received both his Bachelor and M.Sc degrees from Shandong University in China. He is currently working toward his PhD degree in optical communications, at the School of Electric, Electrical and System Engineering of the University of Birmingham. His PhD study is funded by the scholarships from University of Birmingham and Chinese Scholarship Council.

His research interest focuses on the optoelectronic devices, including optical amplifiers, FBG, lasers etc.

H. Ghafouri-Shiraz (S'85–M'86–SM'88) received the B.Sc. and M.Sc. degrees in electronic and electrical engineering from Shiraz University, Shiraz, Iran, in 1973 and 1978, respectively, and the D.Eng. degree from the University of Tokyo, Tokyo, Japan, in 1985.

He is a reader in Optical fibre and Microwave Communications and the Head of postgraduate research studies in the School of Electronic, Electrical, and System Engineering at the University of Birmingham, U.K. Dr Ghafouri-Shiraz research interests include optical communications, optical networks, optical devices, terahertz antenna and filters for medical applications. He has published more than 240 papers all in refereed journals and conferences and is the author of five books including: (i) 'Optical CDMA Networks; Principles, Analysis and Applications' which is published in April 2012 by John Wiley and endorsed by IEEE, (ii) ' The Principles of Semiconductor Laser Diodes and Optical Amplifiers: Analysis and Transmission Line Laser Modelling' published by Imperial College press in 2004 and (iii) 'Distributed Feedback Laser Diodes and Optical Wavelength Tuneable Filters' published by John Wiley in 2003.